Journal of Photochemistry & Photobiology, A: Chemistry 474 (2026) 117005

Contents lists available at ScienceDirect

Journal of Photochemistry & Photobiology, A: Chemistry

journal homepage: www.elsevier.com/locate/jphotochem

Solvatochromic and electronic effects in the photochemical behavior of chalcones and iminochalcones

Beatriz A. Riga-Rocha [a,b,*], José C. Netto-Ferreira [c], Carla C. Schmitt [b], Antonio E.H. Machado [d,e], Thiago F. Silva [e]

[a] Faculdade de Engenharia de Ilha Solteira – Universidade Estadual Paulista, CEP 15385-007 Ilha Solteira, SP, Brazil
[b] Instituto de Química de São Carlos – Universidade de São Paulo (IQSC-USP), CEP 1960-900 São Carlos, SP, Brazil
[c] Instituto de Química – Universidade Federal Rural do Rio de Janeiro, CEP 23970-000 Seropédica, RJ, Brazil
[d] Laboratório de Fotoquímica e Ciência de Materiais, Instituto de Química, Universidade Federal de Uberlândia, CEP 38400-902 Uberlândia, MG, Brazil
[e] Programa de Pós-Graduação em Ciências e Engenharia de Materiais, Instituto de Física, Universidade Federal de Catalão, CEP 75705-220 Catalão, GO, Brazil

ARTICLE INFO

Keywords:
Chalcones
Iminochalcones
Transient spectroscopy
E/Z-photoisomerization
[2_π+2_π] photocycloaddition

ABSTRACT

The transient photophysical properties and the photochemical behavior of a series of chalcone derivatives, nitrochalcone **1a**, aminochalcone **1b**, and *para*-substituted iminochalcones **2a** —$N(CH_3)_2$, **2b** —H, and **2c** —NO_2, were investigated *via* UV–Vis spectroscopy, laser flash photolysis, and density functional theory (DFT) calculations. ^{1}H NMR spectroscopy was utilized to characterize the photoreaction products. Transient lifetimes fall in the nanosecond range, and the absorption wavelength of the transient of all compounds is influenced by the electronic characteristics of the substituents, as well as the solvent properties. Charge-transfer character plays a crucial role in the behavior exhibited by compounds **1b** and **2a**. The stabilization of the intramolecular charge-transfer state for **2a** in acetonitrile completely suppressed its transient formation. The behavior observed for all compounds is consistent with the assignment of the transients as triplet species, as reported for structurally related chalcones in the literature. DFT calculations for triplet absorption spectra, Jablonski diagrams, and symmetry analysis of natural transition orbitals further support this observation. Non-radiative decays commanded the photophysical properties of compounds **1a** and **2c**. All compounds underwent either photoisomerization or photocycloaddition when irradiated at their maximum absorption wavelength (λ_{max}). The molecular structure, solvent properties, and irradiation wavelength all influenced the reactions observed with the chalcones. An *E/Z*-photoisomerization reaction was confirmed for **1a** and **1b** in DMSO, under LED irradiation at $\lambda_{\mathbf{1a}} = 365$ nm and $\lambda_{\mathbf{1b}} = 400$ nm. These results support chalcones as a versatile class of compounds that can be tailored for different applications by fine-tuning their molecular structure, the surrounding medium, and the stimuli for photoreaction.

1. Introduction

Chalcones are a class of molecules known not only for their medicinal properties [1] but also for their capability to undergo photochemical reactions that lead to various other compounds. To illustrate the significance of these photoreactions, it is worth mentioning the improvement that the incorporation of chalcone molecules brought to the development of liquid crystal displays (LCD) [2]. Previously, the mass production of LCDs involved aligning mechanically fine layers of polyimides by rubbing cotton or nylon tissue against the LCD material [3,4]. However, after the incorporation of polymers with photoreactive units, such as polyvinyl cinnamates (PVCi) [5], the alignment process began to be performed through photoisomerization or photodimerization reactions, thereby becoming a process that is free from human contact and allowing the creation of more complex structures [2]. The similarity between the reactivity of cinnamates and chalcones lies in the presence of a conjugated α,β-unsaturated carbonyl system, which allows chalcones also to be employed as photoalignment agents in liquid crystal display devices [6].

Under irradiation, chalcone molecules can populate $S_{\pi\pi^*}$ and $S_{n\pi^*}$ excited states. These compounds can also present a high intersystem crossing (ISC) rate constant [7]. Such characteristics favor the existence

* Corresponding author at: Faculdade de Engenharia de Ilha Solteira – Universidade Estadual Paulista, CEP 15385-007 Ilha Solteira, SP, Brazil.
E-mail address: riga.rocha@unesp.br (B.A. Riga-Rocha).

https://doi.org/10.1016/j.jphotochem.2025.117005
Received 23 August 2025; Received in revised form 16 December 2025; Accepted 18 December 2025
Available online 19 December 2025

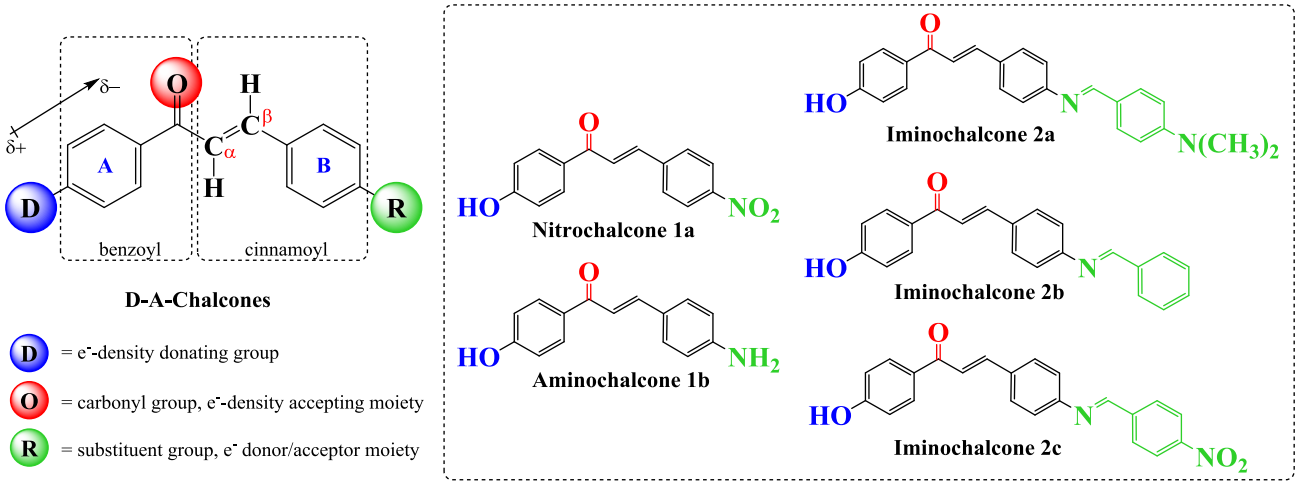

Scheme 1. Illustration of a chalcone molecule highlighting the position of the substituent group and the presence of the donor and acceptor units (left). Representation of the chalcone derivatives investigated in this study (right).

of $S_{\pi\pi^*} \rightarrow T_{n\pi^*}$ and $S_{n\pi^*} \rightarrow T_{\pi\pi^*}$ electronic transitions, leading to the population of triplet states [8]. The possibility of populating different excited states endows chalcones with interesting photoreactive properties. Depending on the structure of the chalcone, especially considering the substituents and their position on the molecule, the compound can undergo different excited-state reactions. A typical example is the photocyclization of the 2′-hydroxychalcone, which enables the obtention of the basic structure of flavones [9,10]. These photoreactions can either occur on the α,β-unsaturation or involve the carbonyl group and a substituent. Among the assortment of photochemical reactions presented by chalcones, photoisomerization (E/Z-isomerization) and photodimerization ($[2_\pi+2_\pi]$ cycloaddition) are the most studied ones, due to their potential to favor the development of better materials, as in the case of LCDs, for instance.

Photodimerization is the name given to a $[2_\pi+2_\pi]$ photocycloaddition between free chalcone molecules. Conversely, when this reaction involves chalcone moieties attached to a polymeric chain, for instance, it is referred to as photo-crosslinking. In both cases, this reaction is characterized by the chemical interaction between an α,β-unsaturated ketone in the triplet excited state and an α,β-unsaturated ketone in the ground state, leading to the formation of a cyclobutane ring that connects them [11]. Depending on the orientation of the α and β carbons during the cycloaddition, there is a possibility of forming four different cyclobutane isomers, known as α- and ε-truxilic, β- and δ-truxinic isomers [12,13].

When a chalcone molecule is irradiated, a photoisomerization reaction of the C=C double bond may occur. This light-triggered process, as observed in disubstituted olefins, can proceed directly from the singlet or triplet states, following two mechanistic pathways: single-path or dual-path [14]. The single-path mechanism occurs exclusively *via* triplet states [15], whereas the dual-path mechanism involves the mutual participation of singlet and/or triplet states [16]. The occurrence of one mechanism over the other, or even the simultaneous occurrence of both, will depend on the stability of the excited states and is directly influenced by the substituents and the surrounding environment.

As presented above, *E/Z*-photoisomerization and $[2_\pi+2_\pi]$ photocycloaddition are chemical reactions that require the population of specific excited states to occur. The distinctive features of these photoreactions and the importance of their physical processes highlight the equal significance of synthesizing new chalcones and examining their photophysical and photochemical properties. Additionally, innovations across multiple scientific fields may arise from advances in understanding these compounds and their associated phenomena. Motivated by this scenery, we present an investigation of the excited state processes of five chalcone derivatives, which differ in the donor-acceptor character of their substituents and whose structures are shown in Scheme 1. Herein, their transient photophysical properties, solvatochromic characteristics, photochemical kinetics, and product characterization are exhibited.

2. Experimental

2.1. Chemicals

All solvents were purchased from Sigma-Aldrich and used without further purification. Methanol (MeOH), acetonitrile (MeCN), and ethyl acetate (EtOAc) were HPLC grade. Chalcones 1-(4-hydroxyphenyl)-3-(4-nitrophenyl)prop-2-en-1-one (**1a**) and 3-(4-aminophenyl)-1-(4-hydroxyphenyl)prop-2-en-1-one (**1b**) and iminochalcones (**2a-c**) were synthesized as previously described [17]. Briefly, nitrochalcone **1a** was prepared through a Claisen-Schmidt condensation reaction involving 4-hydroxyacetophenone and 4-nitrobenzaldehyde. Then **1a** was converted into aminochalcone **1b** by reduction of the -NO_2 group catalyzed by Fe°. Afterwards, **1b** was subjected to a condensation reaction with the respective *p*-substituted benzaldehydes (R = —$N(CH_3)_2$ (**2a**), —H (**2b**), and —NO_2 (**2c**)) to produce iminochalcones **2a-c**.

2.2. Instrumental

UV–Vis measurements were performed on a Shimadzu UV-2550 spectrophotometer in the 500 to 200 nm range, with a spectral resolution of 0.5 nm. Transient decays and triplet-triplet absorption spectra were determined using a Laser Flash Photolysis LUZCHEM mini-system apparatus, model mLPF112. Samples were excited by the third harmonic (λ_{exc} = 355 nm, single pulses of 5.2 ns duration and 40 mJ/pulse) of an Nd-YAG laser Brilliant B, Quantel. The studies were conducted in solutions, using methanol (MeOH), acetonitrile (MeCN), and ethyl acetate (EtOAc) as solvents. The solutions in 1 cm path length quartz cells were degassed by bubbling N_2 (free of O_2) for 15 min and stored under N_2 atmosphere for analysis. The sample concentrations were selected to ensure their absorbances at 355 nm were approximately 0.3. ^{1}H NMR spectra were obtained using an Agilent Technologies 500/54 Premium Shielded in DMSO-d_6 at 25.0 ± 0.1 °C. Chemical shifts were reported in ppm relative to TMS. The steady-state photochemical studies were performed in quartz cells (1 cm path length) using an Oriel 68,805, equipped with an Hg(Xe) ThermoOriel 6292 lamp (200 W) as the light source. The photoreactions accompanied by ^{1}H NMR spectroscopy were conducted in quartz tubes using a multispectral photoreactor, Delpho

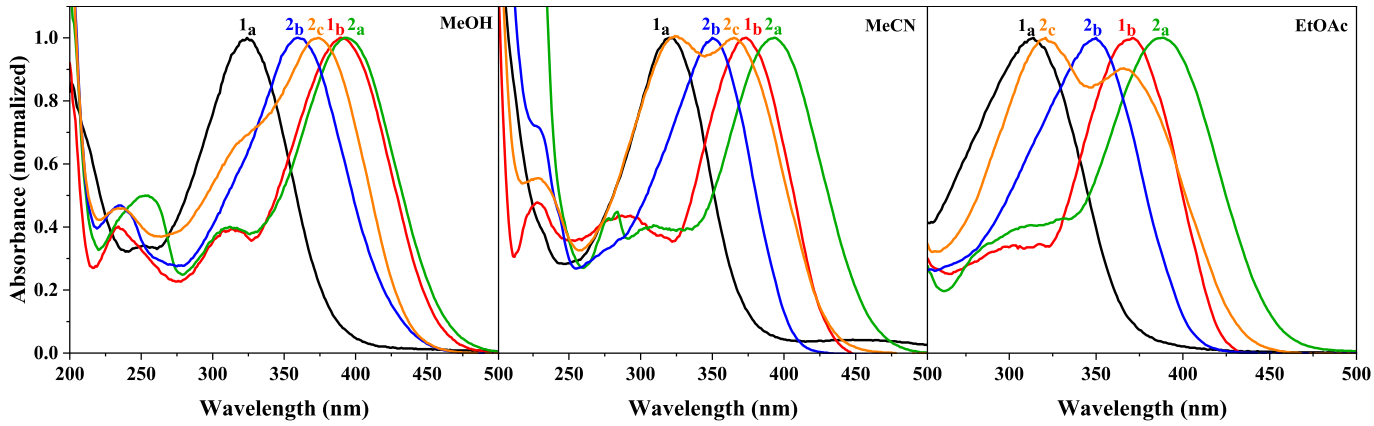

Fig. 1. UV–Vis absorption spectra of nitrochalcone **1a**, aminochalcone **1b**, and iminochalcones **2a**, **2b**, and **2c** [2×10^{-5} M] in MeOH, MeCN, and EtOAc.

Instruments, Multi-Fotons 320RA, equipped with LEDs of different wavelengths (365, 400, 470, 515, 568, 590, and 624 nm) as light sources.

2.3. Data analysis

The percentage of photoconversion was calculated using the equation: photoconversion (%) = $[(A_0 - A_t)/A_0] \times 100$, where A_0 and A_t correspond to the absorbance at the irradiation wavelength before irradiation and after each irradiation interval, respectively. The kinetic rate constants (k_{obs}) correspond to the slope of the linear fit of ln $[(A_0–A_\infty)/(A_t–A_\infty)]$ *vs.* irradiation time, where A_0, A_t, and A_∞ are the absorbances at the irradiation wavelength before irradiation, at a given time t, and at the photostationary state, respectively. Following the methodology reported by Stadler and coworkers [18], the reaction quantum yield ($\Phi_{reaction}$) for the irreversible processes was determined using the equation: $\Phi_{reaction} = (k_{obs} \times C_0)/I_a$, where k_{obs} is the first-order rate constant, C_0 is the initial sample concentration, and I_a is the absorbed light intensity at time zero. For reversible processes, the pseudo total quantum yield (Q, defined as $Q = \varepsilon_Z\Phi_Z + \varepsilon_E\Phi_E$) was calculated according to Stadler and coworkers [18] using the equation: $Q = k_{obs}/(l \times I_0 \times F)$, where k_{obs} is the first-order rate constant, l is the path length of irradiation, and F is the photokinetic factor (defined as $F = (1–10^{-A0})/A_0$, with A_0 being the absorbance at the irradiation wavelength at time zero).

2.4. Theoretical calculations

The ground-state structures of compounds **1a,b**, and **2a-c** were optimized in MeOH, MeCN, and EtOAc, and their vibrational frequencies were subsequently calculated. This optimization was performed using Gaussian G09 [19] with the B3LYP functional [20] in combination with the DGDZVP basis set [21,22]. In the sequence, T_1-state geometries were optimized for each solvent using ORCA 6.1.0 [23,24], employing the B3LYP functional [20] with the def2-TZVPP basis set [25–27] and the Def2-TZVPP/C, which is an auxiliary basis set suitable for post-(CAS)SCF dynamical electron correlation methods, for use with the respective def2 orbital basis [23]. After, the excitation spectra for the first twenty triplet excited states were calculated from the relaxed T_1 geometries using ORCA 6.1.0 [23,24]. The double-hybrid functional B2PLYP [28–30] was used in combination with the def2-TZVPP basis set and the Def2-TZVPP/C auxiliary basis set. In all calculations, the solvents were described using the CPCM model [31,32].

3. Results and discussion

3.1. Photophysical studies – Laser Flash Photolysis (LFP)

The photophysical characterization of the compounds **1a,b**, and **2a-c** began with the analysis of their ground-state absorption spectra, recorded in MeOH, MeCN, and EtOAc solutions. As presented in Fig. 1, chalcones and iminochalcones exhibited a very intense band in the region between 300 and 425 nm. This transition band is attributed to strongly allowed $\pi \rightarrow \pi^*$ transitions, involving mixed $\pi_{cinnamoyl} \rightarrow \pi^*$ and $n_{c=o} \rightarrow \pi^*$ character [33], and presenting a Frank-Condon (FC) excited state with strong intramolecular charge transfer (ICT) character [34]. Two other bands are noticed, especially in MeOH and MeCN. The band around 275 and 300 nm arises from the mixed $\pi_{benzoyl} \rightarrow \pi^*$ and $\pi_{c=o} \rightarrow \pi^*$ transitions. On the other hand, the band below 275 nm is frequently attributed to the $\pi_{Ph} \rightarrow \pi^*$ absorption process in the π-orbitals of the phenyl rings [17]. For compounds **1a**, **1b**, and **2a**, an evident bathochromic shift in polar solvents was observed for the main band, agreeing with the proposed ICT character (Table 1). Iminochalcones **2b** and **2c** also displayed a shift to larger wavelengths, but only considering the polarity change from MeCN to MeOH. Regarding the EtOAc solution, these compounds presented λ_{max} values very similar to those recorded in MeCN. No trend in the molar absorption coefficient (ε_{max}) was observed with changes in solvent polarity.

The technique of Laser Flash Photolysis was employed in the excited-state photophysical characterization of chalcones **1a,b**, and iminochalcones **2a-c**; their photophysical behavior was assessed in MeOH, MeCN, and EtOAc. No transients were observed for iminochalcone **2c** in

Table 1
Ground-state photophysical properties of chalcones **1a,b**, and iminochalcones **2a-c** in solvents of different polarities.

Entry	Chalcone	λ_{max} (nm)			ε_{max} (10^4 M^{-1} cm^{-1})		
		MeOH[a]	MeCN[b]	EtOAc[c]	MeOH[a]	MeCN[b]	EtOAc[c]
1	**1a** (—NO_2)	324	320	314	2.97	2.74	2.48
2	**1b** (—NH_2)	390	374	371	2.99	2.36	2.46
3	**2a** (—$N(CH_3)_2$)	394	394	389	3.08	2.50	4.61
4	**2b** (—H)	360	350	350	3.94	4.11	3.89
5	**2c** (—NO_2)	374	365	366	3.71	3.40	3.15

Relative polarity values from Reichardt and Welton [35]: [a]MeOH = 0.762; [b]MeCN = 0.460; [c]EtOAc = 0.228.

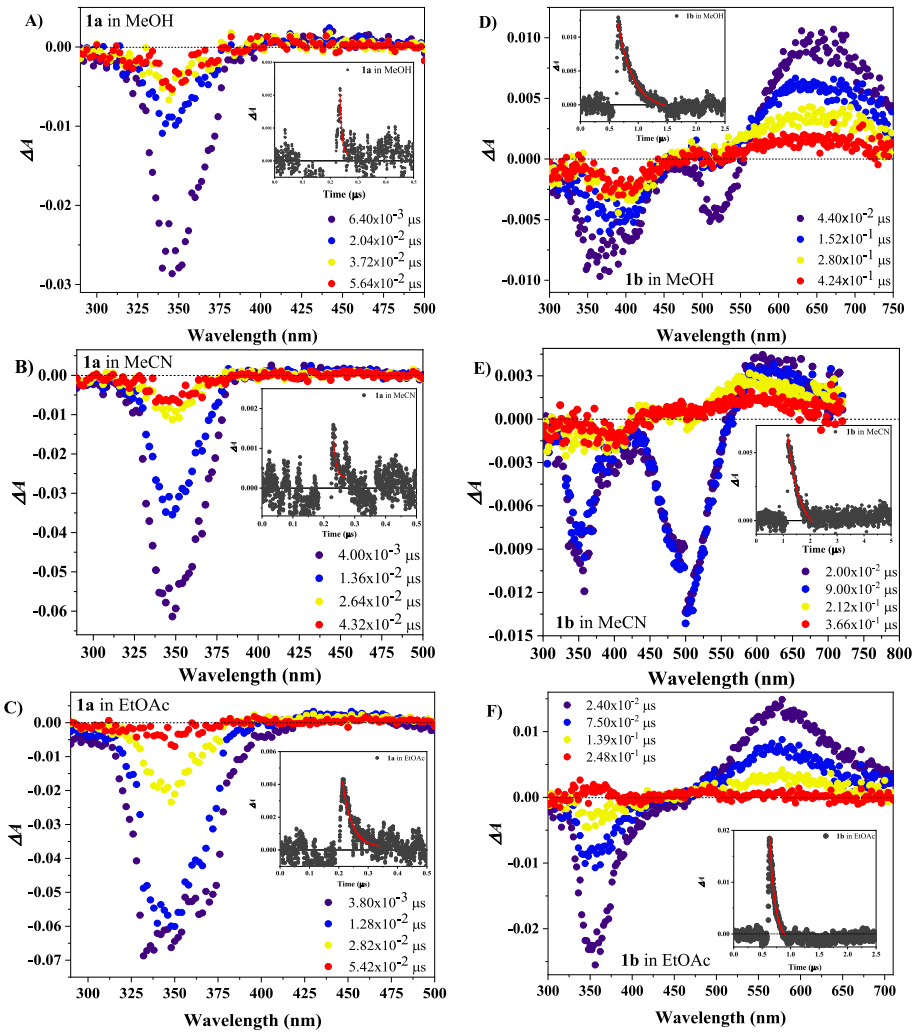

Fig. 2. Transient absorption spectra of **1a** and **1b** acquired at different times after the laser pulse in MeOH, MeCN, and EtOAc; Insert: decay plot for the transient generated from **1a** monitored at **A)** $\lambda_{MeOH} = 440$ nm [3×10^{-5} M], **B)** $\lambda_{MeCN} = 430$ nm [3×10^{-5} M], **C)** $\lambda_{EtOAc} = 430$ nm, [5×10^{-5} M], and from **1b** monitored at **D)** $\lambda_{MeOH} = 650$ nm [1.5×10^{-5} M], **E)** $\lambda_{MeCN} = 610$ nm [1.5×10^{-5} M], **F)** $\lambda_{EtOAc} = 600$ nm, [2×10^{-5} M].

any of these solvents. Decay kinetics for all compounds were fitted considering a monoexponential profile, and the good correlation indicates the occurrence of a unimolecular process.

As presented in Fig. 2-A, 2-B, and 2-C, the transient decay profiles of compound **1a** are accompanied by transient absorption spectra displaying only the band originating from the recovery of ground-state S_0-S_1 absorption. However, the absence of a transient absorption band for **1a** does not imply the absence of species in the excited state, especially when decay profiles (inserted graphs in Fig. 2A-C) were registered and a visible recovery of the S_0-S_1 band over time is observed. In fact, nitroaromatic compounds are known for having many closely packed π-π* and n-π* electronic excited states with different multiplicities that favor intersystem crossing (ISC), and result in efficient triplet formation (large ISC rate constant, k_{ISC}) [36,37]. However, despite favoring the ISC, the presence of the -NO_2 group can also increase the rates of deactivation processes, due to the vibrational modes of the nitro group. Higher deactivation rates (kd) lead to a lower chance of ISC occurrence, so the triplet signal becomes less intense [37].

On the other hand, the transient spectrum of compound **1b** (Fig. 2-D, 2-E, and 2-F) recorded at different times after the laser pulse exhibited a broad band at wavelengths above 550 nm, attributed to a transient absorption process. Furthermore, in MeOH and MeCN (Fig. 2-D and 2-E), this compound exhibited two regions of negative ΔA values, approximately between 330 and 450 nm and at 500 nm, corresponding to the S_0-S_1 absorption and to the S_1-S_0 emission processes, respectively. Meanwhile, only the band at shorter wavelengths is observed in EtOAc (Fig. 2-F). Similar to **1b**, compounds **2a** and **2b** exhibited a broad transient absorption band above 550 nm, along with two negative bands derived from the ground-state absorption and S_1 excited-state emission processes. However, in comparison to **1b**, compound **2a** only featured a transient decay profile in MeOH and EtOAc (Fig. 3-A and 3-B), while compound **2b** only presented a decay profile in MeOH (Fig. 3-C).

It is known that the intersystem crossing (ISC) process for chalcones is highly efficient; thus, it is expected that the population of the triplet excited states $T_{n\pi^*}$ and $T_{\pi\pi^*}$, typical of the enone group [7,8], would be readily observed. The transient maximum absorption wavelengths (λ_{max}^{T-T} values in bold) in Table 2 shows that the higher the electron donor ability of the substituent and the number of conjugated π bonds, the longer the λ_{max}^{T-T} of the transient band. Such an observation corroborates the work of Plotnikov [8], which demonstrated how the conjugated bond chain length and the presence/position of electron-donor/acceptor substituents can influence the arrangement of the states $S_{\pi\pi^*}$, $S_{n\pi^*}$, $T_{\pi\pi^*}$, and $T_{n\pi^*}$. Additionally, Plotinikov's work highlighted the effect of hydrogen bonds and the potential formation of complexes with protic solvents on the arrangement of the ππ* and nπ* states. Regarding the influence of the solvent, our present work registered a bathochromic shift for aminochalcone **1b** as the solvent polarity increased, following the order λ_{max}^{T-T} (EtOAc) = 575 nm < λ_{max}^{T-T} (MeCN) = 610 nm < λ_{max}^{T-T}

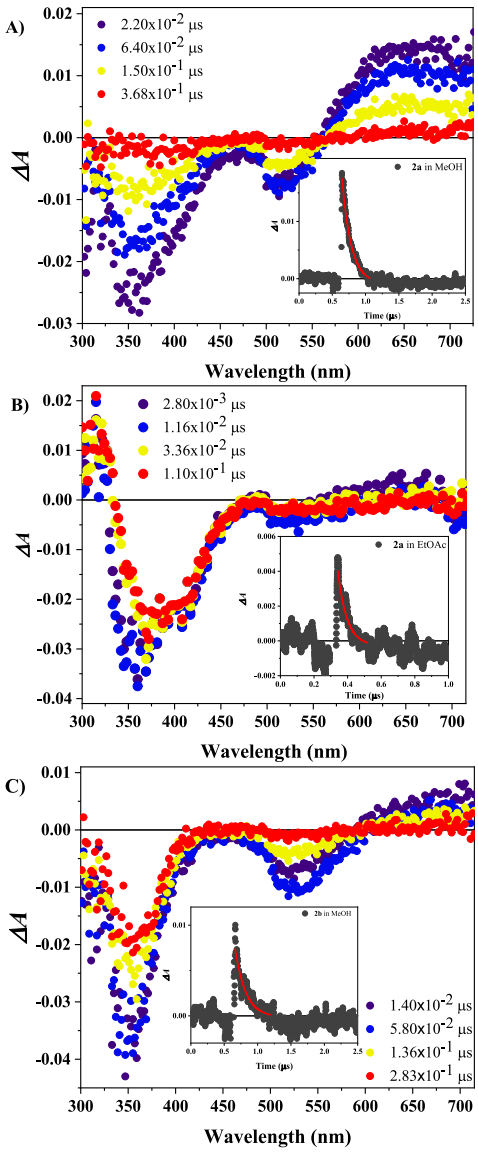

Fig. 3. Transient absorption spectra acquired at different times after the laser pulse for **2a** in **A)** MeOH, **B)** EtOAc, and for **2b** in **C)** MeOH; Insert: decay plot for the transient generated upon irradiation of **2a** at $\lambda_{MeOH} = 670$ nm [1.5×10^{-5} M], and $\lambda_{EtOAc} = 670$ nm, [1×10^{-5} M], and of **2b** at $\lambda_{MeOH} = 650$ nm [9×10^{-6} M].

(MeOH) = 650 nm. Such behavior indicates stabilization of the excited state as the polarity and protic character of the solvents increase (from EtOAc to MeOH), thereby reducing the energy required for the transition. Finally, the susceptibility of this transient band to the substituent electronic effect, the polar/protic character of the medium, and the registered lifetime (τ) values—which will be better discussed ahead—suggest that this transient formation might be associated with the population of a $T_{\pi\pi^*}$ excited state [8,38].

Due to the ultrashort lifetime of the transient species, common triplet quenchers such as O_2 proved ineffective under our experimental conditions. Thus, to aid understanding of triplet formation in these compounds, a Density Functional Theory (DFT) study was carried out, using time-dependent DFT (TD-DFT) to calculate the absorption spectra. The theoretical calculations showed good agreement with the experimental observations for compounds **1b**, **2a**, and **2b**. For the nitro-substituted compounds **1a** and **2c**, due to the presence of the -NO_2 group and the complexity of its excited-state processes, TD-DFT calculations were less effective. The triplet absorption spectra calculated for chalcones **1a,b**, and **2a-c** are presented in Supp. Table S1-S15. As a representative example of the behavior observed for **1b**, **2a**, and **2b**, the theoretical triplet absorption spectrum of **1b** in MeOH is exhibited in Fig. 4A. As can be observed, a very strong transition appears at 413.3 nm ($f_{osc} = 1.235$) and corresponds to the $T_{0\text{-}1A} \rightarrow T_{1\text{-}1A}$ process. This transition is followed by much less intense ones at shorter wavelengths. The analysis of the Jablonski diagram (Fig. 4B) and the contour plots of the natural transition orbitals (NTO) (Fig. 4C)—which present a significant change in symmetry from HOLE S_1 to PARTICLE T_3—indicates the viability of the intersystem crossing. The calculated value of ΔE_{ISC} for compound **1b** is ~3 kJ/mol. This value can be larger depending on the compound, for example, for iminochalcone **2a**, in MeOH, $\Delta E_{ISC} \approx 48{,}4$ kJ/mol as calculated from the Jablonski diagram in Fig. 4D.

Table 2
Transient photophysical properties of compounds **1a,b**, and **2a-c** in solvents of different polarities.

Entry	Compound	Solvent[a]	λ (nm)	τ (ns)	$1/\tau$ (s^{-1})
1		MeOH	440	9.5[b]	1.0×10^8
2	**1a** (-NO_2)	MeCN	430	9.1[b]	1.1×10^8
3		EtOAc	430	9.1[b]	1.1×10^8
4		MeOH	**650**[d]	199.9	5.0×10^6
5			350	204.0	4.9×10^6[c]
6	**1b** (—NH_2)	MeCN	**600**[d]	190.6	5.3×10^6
7			330	83.2	1.2×10^6[c]
8		EtOAc	**575**[d]	65.4	1.5×10^7
9			320	167.9	6.0×10^6[c]
10			**670**[d]	105.7	9.5×10^6
11		MeOH	525	241.3	4.1×10^6[c]
12			350	88.0	1.1×10^7[c]
13	**2a** (—$N(CH_3)_2$)	MeCN	–	–	–
14			**670**[d]	13.5[b]	7.4×10^7
15		EtOAc	525	83.0	1.2×10^7[c]
16			370	157.2	6.4×10^7[c]
17			**650**[d]	143.6	7.0×10^6
18		MeOH	530	48.2	2.1×10^7[c]
19	**2b** (—H)		350	104	9.6×10^6[c]
20		MeCN	–	–	–
21		EtOAc	–	–	–
22		MeOH	–	–	–
23	**2c** (—NO_2)	MeCN	–	–	–
24		EtOAc	–	–	–

[a] Relative polarity values from Reichardt and Welton [35]: MeOH = 0.762; MeCN = 0.460; EtOAc = 0.228.
[b] Lifetime values were calculated from the decay profile at 375 nm.
[c] Rate constants from the recovery processes.
[d] Transient maximum absorption wavelengths λ_{max}^{T-T}.

Although no direct experimental confirmation of a triplet excited state was achieved for chalcones **1a,b**, and **2a,b**, several pieces of indirect evidence support this assignment. First, the transient species observed by laser flash photolysis exhibit lifetimes in the nanosecond range (Table 2), which, although relatively short, are consistent with triplet states of conjugated enones, particularly in systems where efficient non-radiative deactivation or intersystem crossing pathways are operative. Similar short-lived triplet transients have been reported for structurally related compounds in the literature [39]. Additionally, the triplet-triplet absorption band for the chalcones shows notable sensitivity to solvent polarity and electronic substituents on the aromatic rings. This solvatochromic behavior is characteristic of π-π* triplet states ($T_{\pi\pi^*}$) with significant electronic delocalization, whose energy and distribution are perturbed by the local environment [8]. Furthermore, fluorescence measurements revealed very weak emission signals [17], suggesting that deactivation from the singlet excited state is inefficient and that ISC is likely the dominant relaxation pathway, as is typical for α,β-unsaturated carbonyl systems [7]. Finally, the photophysical behavior observed for these chalcones closely parallels that of other chalcone-type molecules, for which triplet excited states have been experimentally confirmed using quenching studies or EPR spectroscopy

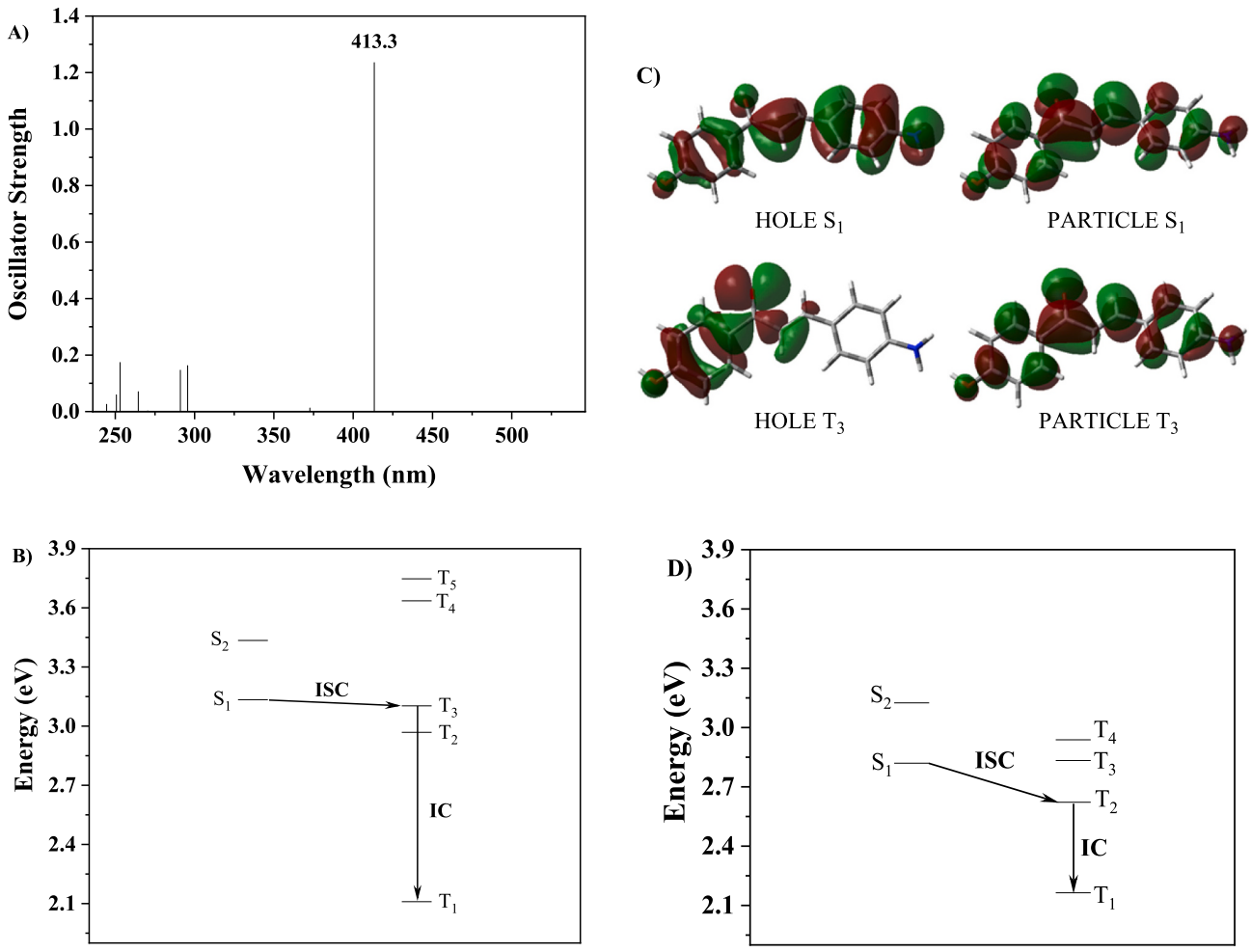

Fig. 4. A) Theoretical triplet absorption spectra of aminochalcone **1b** in MeOH; B) Jablonski diagram calculated for aminochalcone **1b** in MeOH; C) Natural Transition Orbitals (NTO) of S_1 and T_3 states simulated for aminochalcone **1b**; D) Jablonski diagram calculated for iminochalcone **2a**.

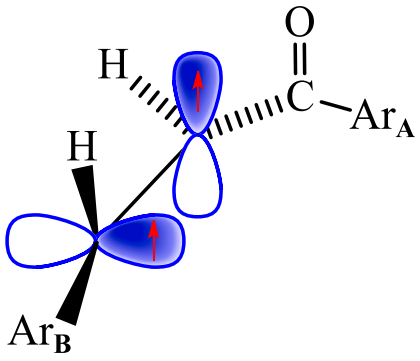

Fig. 5. Representation of the twisted structure for chalcone triplets.

[40]. Taken together, the experimental data, the TD-DFT calculations, and the analogy to structurally similar systems [39,40], provide compelling support for assigning the transient species of compounds **1a, b**, and **2a,b** to a triplet excited state.

As mentioned before, compounds **1a,b**, and **2a,b** exhibited transient lifetimes (τ) in the nanosecond range (Table 2). These values are very similar to those expected for the triplet excited state of chalcones [39]. Comparing the triplet lifetime of chalcones with those of other flavonoids or aromatic ketones, it is easy to notice how chalcones differ from their similar compounds. While chalcones present triplet lifetimes in the order of nanoseconds, flavones and thioxanthones, for example, have these values in the range of microseconds to milliseconds [38,41]. Another interesting fact is that, although the electronic characteristics of the substituents attached to the main structure might not influence the triplet lifetimes, the solvent polarity greatly influences these values. Such behavior is observed for α,β-unsaturated ketones because these compounds, preferably, assume a twisted structure in the triplet excited state, as represented in Fig. 5. This is also why the ISC process of a chalcone molecule is often better understood when compared to those of biradicals or biradicaloid molecules [39].

Comparing the transient lifetimes observed for **2a** and **2b** in methanol (Table 2, entries 10 and 17), it is possible to notice that compound **2a** presented a smaller lifetime. Based on Caldwell and Singh's work [39], one might also have expected that compound **2a** should present a larger τ value than **1b** due to the extension of its *p*-conjugated system and molecular rigidity. However, the opposite is observed here in both cases (see Table 2, entries 4 and 10, 8 and 14), suggesting the presence of competing pathways for **2a**. Considering the structure and previously reported photophysical behavior of compound **2a**, its smaller τ value may arise from the existence of a low-lying intramolecular charge-transfer state (ICT) that funnels energy away from its triplet state [17,34,42]. This hypothesis is supported by the absence of a transient decay for **2a** in MeCN (Table 1, entry 8) and by the fact that in this solvent **2a** presents dual fluorescence, with the more intense fluorescence emission deriving from the ICT state; a characteristic that is not observed in MeOH [17].

The influence of the substituents is also reflected by the non-

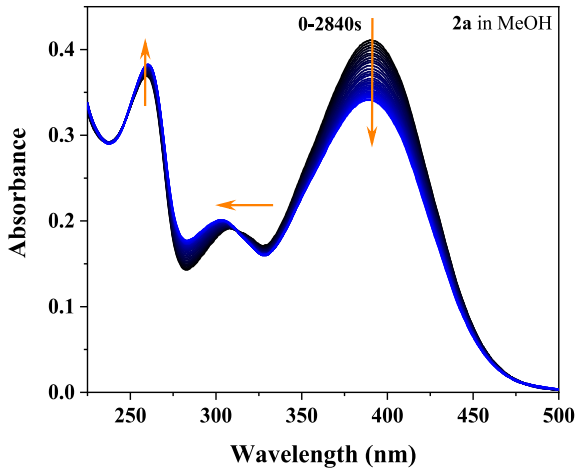

Fig. 6. UV–Vis absorption spectra of iminochalcone **2a** in MeOH [1.5×10^{-5} M], recorded at different time intervals after irradiation with a continuous light beam at 355 nm.

detection of transient decay for **2c** and in the significant difference between the transient lifetimes of **1a** and **1b** (Table 2, entries 1–3 and 4, 6, and 8). These results are related to the fact that *p*-nitro substituted compounds are less prone to populate triplet states and frequently present lifetimes that fall into the sub-nanosecond time domain due to enhanced non-radiative decay [37,43]. The rotation around the bond between the nitro group and the aromatic ring can lead to conical intersections between the excited and ground states, providing non-radiative pathways for efficient internal conversion (IC) [37]. Consequently, the behavior observed for the nitro-substituted compounds **2c** and **1a** corroborates what is presented in the literature for this class of compounds.

Different from the nitro derivatives, the *para*-dimethylamine-substituted chalcones, like compound **1b**, tend to present larger transient lifetimes due to the possibility of forming the lowest triplet state that is more planar around the $C_\alpha = C_\beta$ double bond, featuring elevated charge transfer character [39].

Considering electronic and solvation effects, it was observed that the transient lifetime for **1b** and **2a** in MeOH is longer than that registered for the same compounds in MeCN or EtOAc, which could be explained by the fact that MeOH, as a protic polar solvent, tends to solvate the dipolar structure of the chalcones more effectively in the excited state. A more efficient solvation leads to an increase in the rigidity of the molecule and, consequently, to larger lifetime values for the transient species [44].

3.2. Photochemical studies – kinetics and characterization

During the LFP investigations, a variation in intensity of the ground-state absorption bands of compound **2a** was observed when comparing the UV–Vis spectra acquired before and after the laser pulses at 355 nm. To investigate the nature of the spectral changes, the UV–Vis absorption spectrum was registered at different time intervals to monitor spectral changes until the photostationary state was reached.

As shown in Fig. 6, under irradiation at 355 nm, the band at 390 nm, which is attributed to a mixed $^1(\pi_{cinnamoyl}\text{-}\pi^*)$ and $^1(n_{c=o}\text{-}\pi^*)$ transition, decreases at the same time as the band at 269 nm, assigned to the $^1(\pi_{Ph}\text{-}\pi^*)$ transition, increases. A slightly hypsochromic shift is observed for the band at 390 nm. In contrast, a more pronounced hypsochromic shift is observed for the band at 310 nm, attributed to a mixed $^1(\pi_{benzoyl}\text{-}\pi^*)$ and $^1(\pi_{C=O}\text{-}\pi^*)$ transitions. These spectral changes give rise to an isosbestic point at 313 nm. These observations indicate that the iminochalcone **2a** underwent a photoreaction under irradiation at 355 nm.

After identifying that an excited-state reaction was taking place for **2a**, all compounds were submitted to a photochemical study in which their solutions were irradiated with a continuous light beam at the λ_{max} of the $^1(\pi\text{-}\pi^*)$ transition from $>C_\alpha = C_\beta<$, in MeOH, MeCN, and EtOAc.

Under irradiation, all compounds (**1a,b**, and **2a-c**) exhibited spectral changes. In some cases, such as for chalcones **1a** (Suppl. Fig. S1) and **1b** (Suppl. Fig. S2), these changes were highly expressive, allowing us to study the reaction kinetics. Conversely, for iminochalcones **2a** (Suppl. Fig. S3) in MeCN, and **2b** (Suppl. Fig. S4) or **2c** (Suppl. Fig. S5) in MeCN and EtOAc, the spectral changes were not significant enough, making it difficult to even determine whether the reaction occurred or not.

Under irradiation at their λ_{max}, compounds **1a** and **2a-c** showed a decrease in intensity for the band associated with the $\pi \rightarrow \pi^*$ transition (above 300 nm). This consumption was accompanied by a hypsochromic shift of the same band and/or its neighboring band at a lower wavelength (around 250–300 nm). Observations like these are often seen in molecules that experience a decrease in the extent of their π-conjugation. Additionally, an intensity increase was observed for the band with the highest energy, leading to the appearance of an isosbestic point between this band and the $\pi \rightarrow \pi^*$ band (~300 nm). Such spectral behavior, observed for compounds **1a** and **2a-c**, suggests that these molecules participate in a photoreaction that involves the $>C_\alpha = C_\beta <$ bond. It is worth mentioning that the spectral changes observed for these compounds were mainly irreversible. The samples did not revert to their original form, whether exposed to irradiation at the λ_{max} of the intensified band or kept in the dark. The consumption of the main absorption band as a function of irradiation time is presented in terms of percentage of photoconversion. For all compounds, the percentage of photoconversion was calculated using the equation: photoconversion (%) = $[(A_0 - A_t) / A_0] \times 100$, where A_0 and A_t represent the absorbance at the λ_{max} of the chalcones before starting irradiation and after each irradiation period, respectively. In Fig. 7 and Suppl. Fig. S2-S5, it is observed that the reaction undergone by compounds **1a,b**, and and **2a-c** exhibits an increase in photoconversion after the initial irradiation times, levelling off, eventually, into a plateau. All chalcones and iminochalcones presented a linear dependence of ln $[(A_0\text{-}A_\infty)/(A_t\text{-}A_\infty)]$ *vs.* irradiation time, indicating that **1a,b**, and **2a-c** underwent a photochemical reaction following first-order kinetics (inserted plots in Fig. 7 and Suppl. Fig. S2-S5). Table 3 summarizes the data from these photoreactions.

Apart from what was observed for compounds **1a** and **2a-c**, the aminochalcone **1b** appeared to undergo two different photoreactions, depending on the solvent used in this study. In MeOH, **1b** behaved similarly to the other compounds (Fig. 8A). However, in MeCN and EtOAc, **1b** exhibited the consumption of the $\pi \rightarrow \pi^*$ band (~370 nm) combined with an intensification of the band at 280 nm and the appearance of an isosbestic point around 300 nm (Fig. 8B and C). Another fundamental difference between **1b** and the other compounds is the reversibility of their photoreaction in MeCN and EtOAc. Although reversibility by removing the irradiation light source has not been observed, the reaction was partially reverted by irradiating the solution at the λ_{max} of the intensified band (280 nm). This reversibility study was carried out after **1b** reached the photostationary state; the corresponding absorption spectra are shown in Suppl. Fig. S6.

Regarding the photochemistry of chalcone molecules, it is well known that the consumption of their main band in the 325–400 nm region ($\pi_{cinnamoyl} \rightarrow \pi^*$ and $n_{c=o} \rightarrow \pi^*$ transition) can be caused by two distinct photochemical reactions: $[2_\pi+2_\pi]$ cycloaddition and/or *E/Z*-isomerization [45–49]. When a $[2_\pi+2_\pi]$ photocycloaddition is considered, the intensity decrease of the main band for chalcone molecules comes from the cleavage of the $>C_\alpha = C_\beta <$ bond, followed by the formation of a cyclobutane ring. Once the double bond is broken, the π-conjugation of the chalcone molecule is reduced, frequently shifting the absorption maximum to a shorter wavelength. Beyond that, a gradual increase in the intensity for the band in the 200–250 nm region ($\pi_{benzoyl} \rightarrow \pi^*$ and $\pi_{C=O}\text{-}\pi^*$ transition) is also expected, leading to the appearance of an isosbestic point between this band and that around

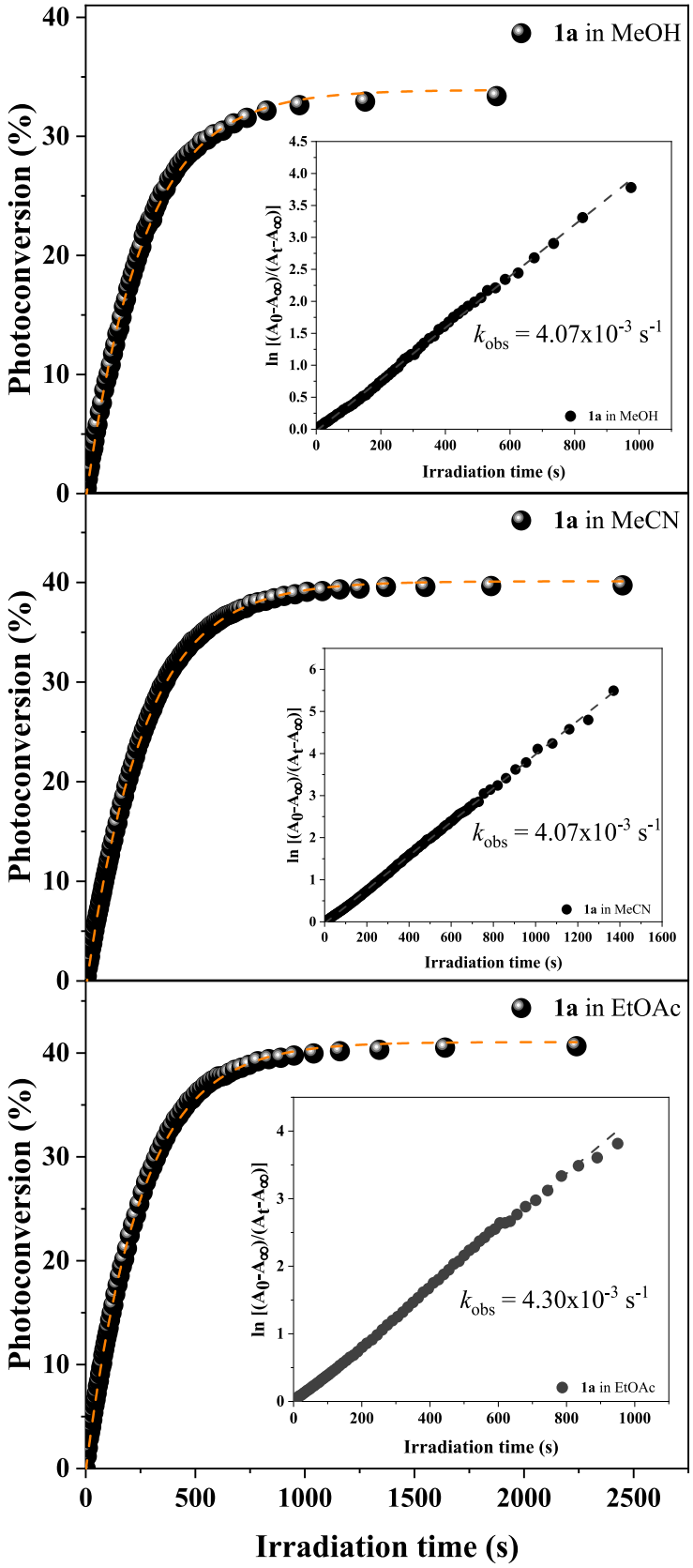

Fig. 7. Percentage of photoconversion *vs.* time and kinetic plot of ln $[(A_0\text{-}A_\infty)/(A_t\text{-}A_\infty)]$ *vs.* time (inserted) of **1a** in MeOH [2.5×10^{-5} M], MeCN [4×10^{-5} M], and EtOAc [5×10^{-5} M]. MeOH: $\lambda_{irr} = 324$ nm, MeCN and EtOAc: $\lambda_{irr} = 324$ nm.

Table 3
Photoreaction data for compounds **1a,b**, and **2a-c** in different solvents.

Entry	Compound	Solvent	λ_{irr} (nm)	Time (s)	Conv. (%)	k_{obs} (10^{-3} s^{-1})	$\Phi_{reaction}$ (10^{-4}) or Q (L Mol^{-1} cm^{-1})[b]
1	**1a** (—NO_2)	MeOH	324	1875	33	4.07	4.22
2		MeCN	322	2450	40	4.01	6.12
3		EtOAc	322	2240	41	4.30	8.02
4	**1b** (—NH_2)	MeOH	390	3670	14	6.06	2.39
5		MeCN	374 280	2681 3785	32 16	28.23 5.13	25.31[b]
6		EtOAc	371 280	1776 1445	23 11	17.43 4.31	19.14[b]
7		MeOH	393	8030	31	0.34	0.09
8	**2a** (—$N(CH_3)_2$)	MeCN	393	5270	—[a]	—[a]	—[a]
9		EtOAc	389	6710	5	0.40	0.07
10		MeOH	360	1740	13	7.47	1.33
11	**2b** (—H)	MeCN	350	1800	—[a]	—[a]	—[a]
12		EtOAc	350	1800	—[a]	—[a]	—[a]
13		MeOH	369	9480	13	0.20	0.05
14	**2c** (-NO_2)	MeCN	365	1800	—[a]	—[a]	—[a]
15		EtOAc	366	1800	—[a]	—[a]	—[a]

[a] At these conditions, either no reaction occurred or proceeded at low extension, which prevented the kinetic monitoring.
[b] Pseudo total quantum yield ($Q = \varepsilon_Z\Phi_Z + \varepsilon_E\Phi_E$) [18], calculated for entries 5 and 6, considering the occurrence of a photochemical *E/Z*-isomerization.

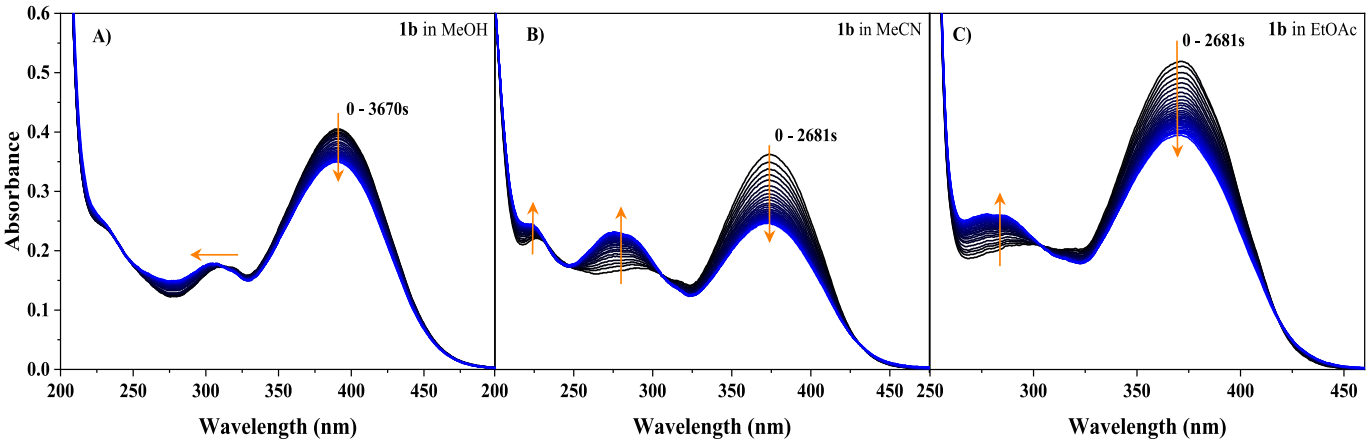

Fig. 8. UV–Vis kinetic monitoring of the photoreaction of **1b** in A) MeOH [1.5×10^{-5} M], B) MeCN [1.5×10^{-5} M], and C) EtOAc [1.5×10^{-5} M]. MeOH: $\lambda_{irr} = 390$ nm, MeCN: $\lambda_{irr} = 374$ nm, and EtOAc: $\lambda_{irr} = 371$ nm.

250–325 nm ($\pi_{cinnamoyl} \rightarrow \pi^*$ transition) [48–50].

On the other hand, when a chalcone molecule is involved in an *E/Z*-photoisomerization, the intensity decrease observed for the main band (around 400 nm) derives from the conversion of the *E*-isomer (*trans-s-cis*- or *trans-s-trans*-chalcone) into its *Z*-isomer (*cis-s-cis*-chalcone). In this case, the relative intensity of the ~325–400 and ~ 250–325 nm bands might change depending on the relative proportion between the isomers. When the most stable isomer (*E*-chalcone) is present in relatively higher concentration, the intensity of the band from the mixed $\pi_{cinnamoyl} \rightarrow \pi^*$ and $n_{c=o} \rightarrow \pi^*$ transition (~325–400 nm) is favored. However, an increase in the concentration of the less stable isomer (*Z*-chalcone) leads to an intensification of the band from the $\pi_{cinnamoyl} \rightarrow \pi^*$ transition (~250–325 nm) and the appearance of an isosbestic point [45,51–53]. Once a chalcone assumes the *Z* isomeric form, the proximity of its carbonyl oxygen and cinnamoyl aromatic ring reduces the planarity of the molecule due to repulsion effects. Nonetheless, the hypsochromic shift for the main band is subtle or even unnoticeable in this case, because there is no effective cleavage of the $>C_\alpha = C_\beta <$ bond. Depending on the stability of the *E/Z* isomers, the back reaction from *Z* to *E* can occur *via* thermal relaxation [45]. However, there are cases in which this conversion does not occur naturally [53]. Under these circumstances, irradiation of the sample at the maximum wavelength of the band around ~250–325 nm can provide enough energy for the $Z \rightarrow E$ isomerization to occur [6,54].

Considering the discussion above and the absorption spectra of all compounds, the [2_π+2_π] cycloaddition is inferred to be the main reaction observed for **1a** and **2a-c**. For compound **1b**, this reaction is also observed, but only in MeOH. On the other hand, in MeCN and EtOAc, compound **1b** appears to undergo *E/Z*-isomerization predominantly. To confirm the occurrence of these two reactions, chalcones **1a** and **1b** were chosen as the respective representatives from the plausible [2_π+2_π]

Table 4
Photoreaction data of compounds **1a,b** and **2a-c** in DMSO.

Entry	Compound	λ_{irr} (nm)	Time (s)	Conv. (%)	k_{obs} (10^{-3} s^{-1})	$\Phi_{reaction}$ (10^{-4}) or Q (L Mol^{-1} cm^{-1})
1	**1a** (—NO_2)	335	2260	37	4.38	2.10
2	**1b** (—NH_2)	400 298	450 975	30 14	18.01 6.02	19.03[b]
3	**2a** (—$N(CH_3)_2$)	406	1120	—[a]	—[a]	—[a]
4	**2b** (—H)	360	2140	—[a]	—[a]	—[a]
5	**2c** (—NO_2)	377	1060	—[a]	—[a]	—[a]

[a] Under these conditions, either no reaction occurred, or it proceeded to a low extension, preventing kinetic monitoring.
[b] Pseudo total quantum yield ($Q = \varepsilon_Z\Phi_Z + \varepsilon_E\Phi_E$) [18], calculated for **1b**, considering the occurrence of a photochemical *E/Z*-isomerization.

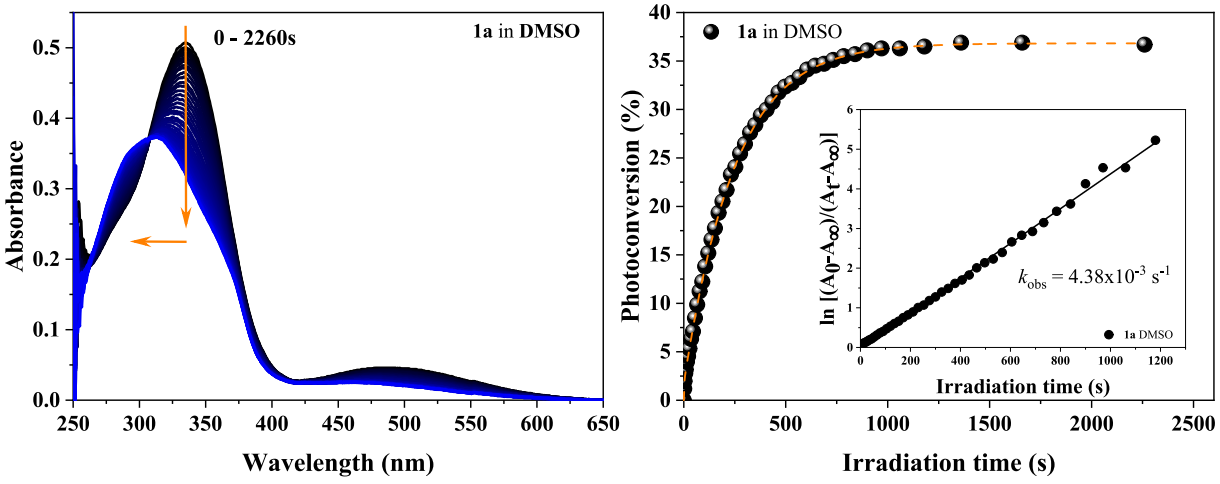

Fig. 9. UV–Vis kinetic monitoring of the photoreaction of **1a** [2×10^{-5} M] ($\lambda_{irr} = 335$ nm), in DMSO. Left: absorption spectra acquired at different irradiation times. Right: respective percentage of photoconversion *vs.* time and kinetic plot of ln [$(A_0-A_\infty)/(A_t-A_\infty)$] *vs.* time (inserted).

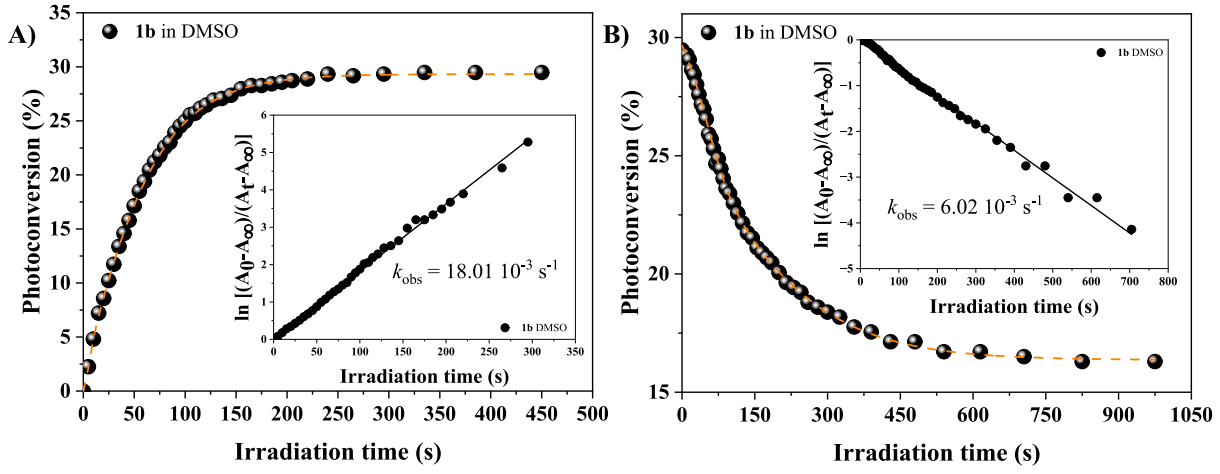

Fig. 10. Percentage of photoconversions *vs.* time and kinetic plot of ln [$(A_0-A_\infty)/(A_t-A_\infty)$] *vs.* time (inserted) for the photoreaction of **1b** [2×10^{-5} M], in DMSO, **A)** irradiated at 400 nm and then **B)** irradiated at 298 nm.

cycloaddition and *E/Z*-isomerization photoreactions. Then, a new irradiation study was conducted, during which the ^{1}H NMR spectra of the compounds were acquired before and after irradiating the samples. For the NMR measurements, the samples were irradiated for 30 min in DMSO-d_6 in quartz tubes using a photoreactor equipped with LEDs ($\lambda_{irr,\mathbf{1a}} = 365$ and $\lambda_{irr,\mathbf{1b}} = 400$ nm). On the other hand, for kinetic studies, the samples in DMSO were irradiated in quartz cells using a Hg (Xe) lamp ($\lambda_{irr,\mathbf{1a}} = 335$ nm and $\lambda_{irr,\mathbf{1b}} = 400$ and 298 nm, selected with a monochromator). This same experiment was conducted for the iminochalcones **2a-c**; however, these compounds did not photoreact in DMSO (see Suppl. Fig. S7). In turn, chalcones **1a** and **1b** presented a linear dependence of ln [$(A_0-A_\infty)/(A_t-A_\infty)$] *vs.* irradiation time, indicating that their photochemical reaction followed first-order kinetics. The results from the kinetic studies in DMSO are summarized in Table 4.

Upon steady-state irradiation of compounds **1a** and **1b** in DMSO ($\lambda_{irr,\mathbf{1a}} = 335$ nm and $\lambda_{irr,\mathbf{1b}} = 400$ nm), the formation of a [$2\pi+2\pi$] photocycloaddition product was observed for nitrochalcone **1a**. In contrast, aminochalcone **1b** underwent *E/Z*-photoisomerization. As presented in Fig. 9, UV–Vis monitoring of compound **1a** irradiation showed the consumption of the band attributed to the $>C_\alpha = C_\beta <$ bond (from the mixed $\pi_{cinnamoyl} \rightarrow \pi^*$ and $n_{c=o} \rightarrow \pi^*$ transition, at 335 nm), followed by a hypsochromic shift, suggesting the cleavage of the π bond and interruption of the conjugation. The photoconversion profile of **1a** (Fig. 9) exhibited a rapid increase in conversion until 500 s, followed by a plateau. The linear fit of ln [$(A_0 - A_\infty)/(A_t - A_\infty)$] *vs.* irradiation time agrees with a first-order kinetics model, with a rate constant (k_{obs}) of 4.38×10^{-3} s^{-1}.

Aminochalcone **1b**, in turn, showed the consumption of the $>C_\alpha = C_\beta <$ band (400 nm), accompanied by an intensity increase of the band assigned to $\pi_{cinnamoyl} \rightarrow \pi^*$ transition (298 nm), revealing an isosbestic point at 316 nm (Suppl. Fig. S8 A). Additionally, upon steady-state irradiation at 298 nm, **1b** demonstrated, to some extent, the reversibility of the photoreaction. This reversibility was not due to a thermal process; it was achieved solely through a photochemical route. Upon irradiation at the maximum absorption wavelength of the $\pi_{cinnamoyl} \rightarrow \pi^*$ transition band (298 nm), this band presented a decrease in its intensity, followed by the intensification of the $\pi_{cinnamoyl} \rightarrow \pi^*$ and $n_{c=o} \rightarrow \pi^*$ absorption band (Suppl. Fig. S8B). Such observations suggest the occurrence of an *E/Z*-photoisomerization for **1b**, followed by the return from *Z* to *E*, *via* photochemical reaction. For the forward reaction (*E* → *Z*), compound **1b** exhibited a photoconversion profile (Fig. 10A) showing a rapid increase in conversion during the initial phase (until 150 s), followed by a plateau, reaching the photostationary state at 30 % of photoconversion. Conversely, the analysis of the reverse reaction (*Z* → *E*) (Fig. 10B) revealed a decrease in the photoconversion values with the appearance of a plateau after 300 s. Both forward and reverse

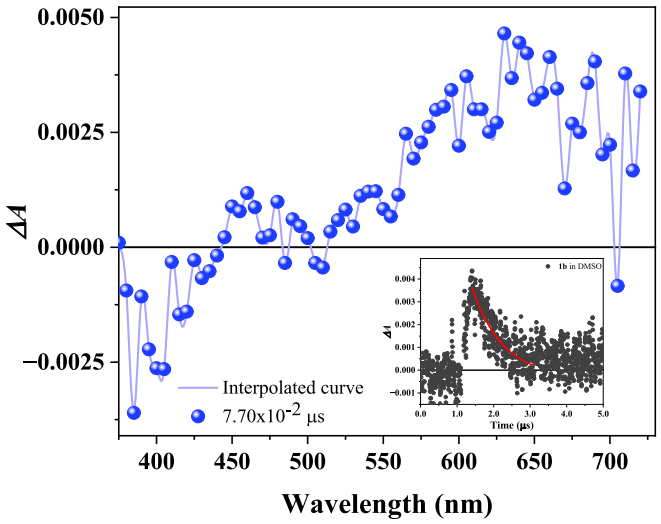

Fig. 11. Transient absorption spectrum of **1b** acquired at 7.70×10^{-2} μs after the laser pulse in DMSO; Insert: decay plot for the transient generated from **1b** upon irradiation at $\lambda_{DMSO} = 650$ nm [2×10^{-5} M].

reactions followed first-order kinetics, as evidenced by the linear relationship between ln $[(A_0 - A_\infty)/(A_t - A_\infty)]$ *vs.* irradiation time, yielding rate constants of 18.01×10^{-3} s^{-1} and 6.02×10^{-3} s^{-1}, respectively.

To aid in understanding the photochemical behavior of compounds **1a** and **1b**, their photophysical characteristics were investigated by laser flash photolysis in DMSO. Unlike what was observed in other solvents, nitrochalcone **1a** in DMSO did not show a transient decay profile. On the other hand, aminochalcone **1b**, under these conditions, generated a transient species with the longest lifetime value among all the compounds ($\tau = 626$ ns; $1/\tau = 1.6 \times 10^8$ s^{-1}). The transient spectrum of compound **1b**, presented in Fig. 11, depicts a broadband, indicative of the transient absorption process, with a maximum near 650 nm. Due to the very low signal intensity, only the spectrum acquired at 7.70×10^{-2} μs after the laser pulse is presented for this compound.

Considering the characteristics of the species in the excited state and the photochemical process presented by aminochalcone **1b**, it is suggested that this compound undergoes an *E/Z*-photoisomerization following the two-way mechanistic path; which may proceed either by singlet or triplet states. Such an indication derives from the following observations: i) the transient lifetime falls in the range of nanoseconds, similarly to the triplet state of olefins that follow this mechanism; ii) the mixture of *E*- and *Z*-isomers in the composition of the photostationary state; and iii) the reversibility of the photoreaction, despite not restoring the initial composition. These characteristics differ from those expected for the adiabatic one-way photoisomerization; i) which proceeds solely on the triplet surface of species with lifetimes longer than nanoseconds, ii) presents a photostationary state formed predominantly by one compound, and iii) is not reversible, mainly by thermal means [14,15,55]. In this study, the reversibility from the *Z*- to the *E*-isomer was triggered by irradiation. The proposal of the two-way mechanistic path for **1b** assumes that thermal relaxation (*via* singlet surface) was possible, even though it was not observed. Therefore, the need for irradiation to initiate the reverse isomerization reaction indicates that, although thermal relaxation is possible, room temperature alone cannot overcome the energy barrier between the two **1b**-isomers, leading the photoreaction to proceed on the triplet surface [56].

Following the observation that compounds **1a** and **1b** exhibit $[2_\pi+2_\pi]$ cycloaddition and *E/Z*-isomerization photoreactions under irradiation in DMSO, a ^{1}H NMR spectroscopy analysis was conducted to investigate this behavior further. Due to experimental limitations, a photoreactor equipped with LEDs (Delpho Instruments) was utilized to irradiate the quartz NMR tubes, instead of the irradiation system (Oriel) used for quartz cells (see the Instrumental section for more details). Although the irradiation experiment did not reproduce the same conditions precisely, the reactions were investigated using the NMR technique. The ^{1}H NMR data for **1a** and **1b** are summarized in Table 5, and their spectra are presented in Suppl. Fig. S9 and S10.

Table 5
Values of chemical shift and coupling constants for the ^{1}H NMR spectra of chalcones **1a** and **1b**, before and after irradiation.

Compound	Group	Before irradiation		After irradiation	
		Signal/δ ^{1}H (ppm) (atom)	*J* (Hz)	Signal/δ ^{1}H (ppm) (atom)	*J* (Hz)
1a (-NO_2)	*meta*-CH (PhOH)	*d* 6.88 (a)	9.0	*d* 6.82 (a)	9.0
	α-CH	*d* 7.71 (b)	15.6	*d* 6.98 (b)	12.8
	β-CH	*d* 8.07 (c)	15.2	*d* 7.05 (c)	12.8
	ortho-CH ($PhNO_2$)	*d* 8.10 (d)	9.0	*d* 7.54 (d)	9.0
	ortho-CH (PhOH)	*d* 8.12 (e)	9.0	*d* 8.81 (e)	9.0
	meta-CH ($PhNO_2$)	*d* 8.24 (f)	9.0	—[a]	—[a]
	OH	*s* 10.50 (g)	–	*s* 10.50 (g)	–
1b (-NH_2)	NH_2	*s* 5.80 (a)	–	*s* 5.59 (a)	–
	meta-CH ($PhNH_2$)	*d* 6.58 (b)	8.5	*d* 6.44 (b)	9.0
	meta-CH (PhOH)	*d* 6.85 (c)	8.5	*d* 6.81 (c)	8.5
	α-CH	*d* 7.50 (d)	15.50	*d* 6.45 (d)	13.00
	ortho-CH ($PhNH_2$)	*d* 7.52 (e)	8.5	*d* 7.44 (e)	8.5
	β-CH	*d* 7.54 (f)	15.50	*d* 6.70 (f)	13.00
	ortho-CH (PhOH)	*d* 7.98 (g)	8.5	*d* 7.82 (g)	8.5
	OH	*s* 10.26 (h)	–	*s* 10.26 (h)	–

[a] These nuclei signals were shifted to regions where a signal overlap occurred (possibly between 8.05 and 8.15 ppm), making it impossible to identify the doublet.

Due to the structural changes undergone by chalcone molecules after isomerization processes or cleavage of the $>C_\alpha = C_\beta<$ bond, the resulting species can be readily identified by ^{1}H NMR spectroscopy through significant alterations in the hydrogen signals and the coupling constants ($^3J_{CH\alpha=CH\beta}$) corresponding to the H_α and H_β pair. In the case of chalcones undergoing an *E/Z*-isomerization, before the reaction starts, the ^{1}H NMR spectrum exhibits the signals of the vinylic H_α and H_β at lower-frequency regions (higher ppm), due to greater deshielding of the nuclei resulting from efficient conjugation in the *E* isomeric form. However, upon the formation of the *Z* isomer, in which conjugation is reduced due to steric effects and decreased planarity, the shielding of the H_α and H_β nuclei increases, and their signals shift to high-field regions (lower ppm). With this conformational change, the coupling constants, which range between 14 and 18 Hz in the *E* isomer, decrease to values between 7 and 12 Hz for the *Z*-isomer [57–59]. On the other hand, if the chalcones undergo a $[2_\pi+2_\pi]$ cycloaddition reaction, the doublet signals arising from the vinylic hydrogens will be consumed and replaced by two new signals with chemical shifts between 3.5 and 5 ppm. The multiplicity pattern for these signals may vary depending on the type of cyclobutane formed. If the cyclobutane system is of the ε-truxillic type (*anti*-head-to-tail), the signals will correspond to triplets. For the α-truxillic (*syn*-head-to-tail) and *δ*-truxinic (*anti*-head-to-head) systems, the signals will resemble multiplets. Finally, if the resulting system is of the β-truxinic type (*syn*-head-to-head), the observed signal will correspond to a multiplet similar to a doublet of triplets [60,61].

Keeping these characteristics in mind and analyzing the hydrogen nuclear magnetic resonance spectra of chalcones **1a** and **1b**, it was possible to observe that the compounds exhibited only evidence of the *E/Z*-isomerization reaction. The ^{1}H NMR spectra did not present the signals expected for the formation of a cyclobutane ring. Conversely, they displayed a shift to higher-frequency regions for the signals of all

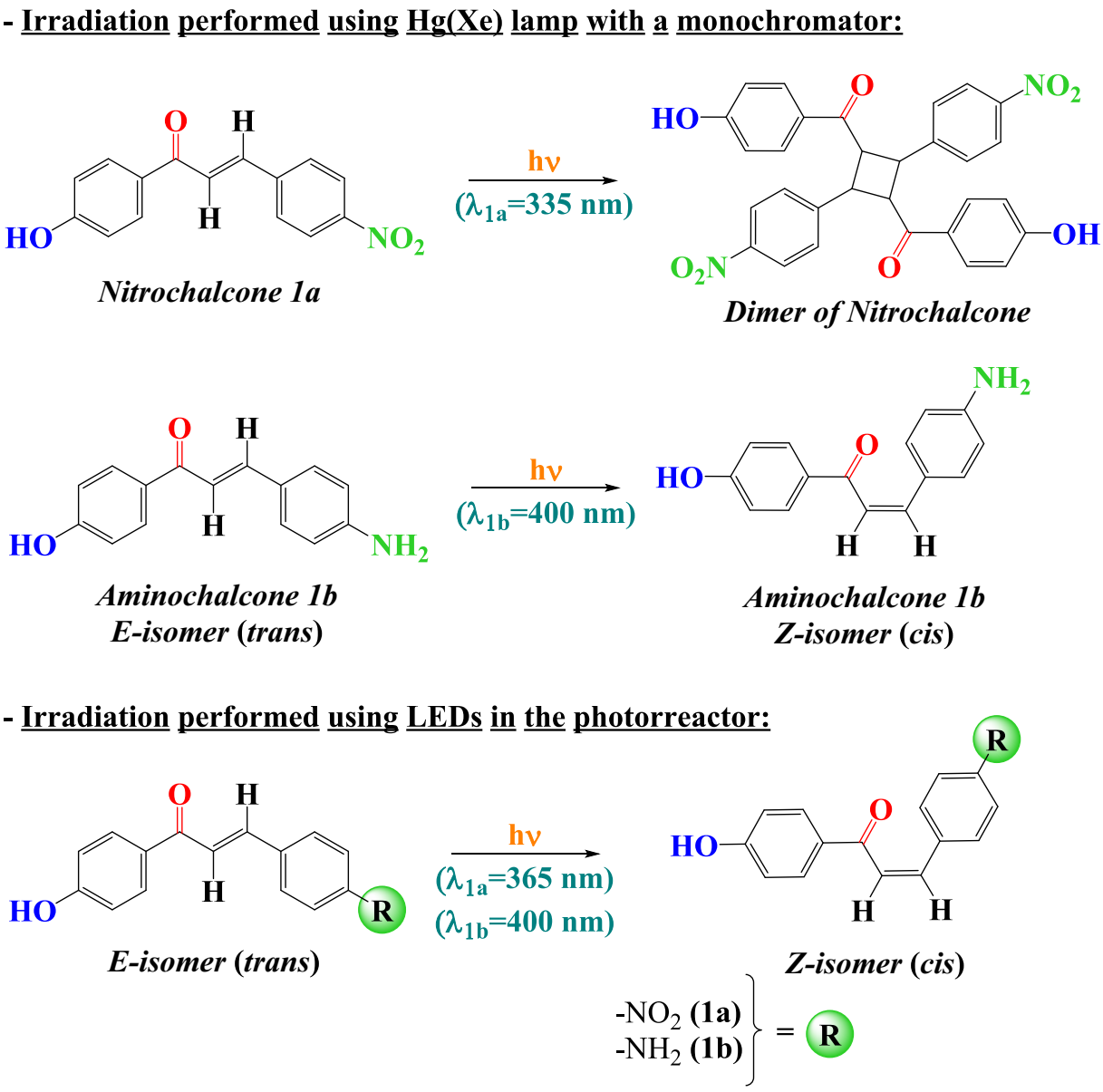

Scheme 2. Illustration of the photoisomerization reaction observed for chalcones **1a** and **1b** after irradiating the samples using an Hg(Xe) lamp (at $\lambda_{1a} = 335$ nm and $\lambda_{1b} = 400$ nm) and LEDs (at $\lambda_{1a} = 365$ nm and $\lambda_{1b} = 400$ nm).

hydrogens (except for the phenolic ones), indicating an increased nucleus shielding (Suppl. Fig. S9 and S10). Furthermore, the coupling constants for the H_α and H_β signals, which initially presented values of 15.6 and 15.5 Hz, for **1a** and **1b**, respectively, after the irradiation assay, changed to 12.8 and 13.0 Hz, confirming the formation of the *Z*-isomer in this assay.

These observations differ from what was expected based on the UV–Vis spectra from the irradiation experiments. The use of distinct irradiation systems, which vary either in the light source's power output or in irradiance of the light source, may be the reason for the divergence in the type of reaction presented by compounds **1a** and **1b** under NMR analysis. Furthermore, whereas the Oriel irradiation system is equipped with an Hg(Xe) lamp and a monochromator, allowing the selection of the exact λ_{max} for irradiation, the Delpho Instruments photoreactor has LEDs, which provide irradiation at specific, predefined wavelengths. Considering this aspect for compound **1b** $\lambda_{max} = \lambda_{irr} = 400$ nm did not cause any problem. However, for compound **1a** $\lambda_{max} < \lambda_{irr}$ (335 nm < 365 nm), which means that the frequency used to irradiate, and consequently, the energy received for **1a**, was inferior to that used in the first experiment. The $[2_\pi+2_\pi]$ cycloaddition reaction requires more energy to occur compared to the *E/Z* isomerization because it involves bond cleavage. Therefore, it is natural to expect that, if the necessary energy is not provided, this reaction does not take place. Hence, it is very plausible that, in the kinetic irradiation experiments, a photocycloaddition was indeed observed for nitrochalcone **1a**. However, when **1a** was irradiated in the photoreactor, photoisomerization was favored due to the equipment features, as observed in the ^{1}H NMR spectrum. For generalization purposes, an illustration of the photoreactions is provided in Scheme 2.

4. Conclusions

Nitrochalcone **1a**, aminochalcone **1b**, and iminochalcones **2a**, **2b**, and **2c** (*p*-substituted with —$N(CH_3)_2$, —H, and —NO_2, respectively), had their transient photophysical, solvatochromic, and photochemical properties investigated. All compounds exhibited transient lifetimes in the 9–200 ns range, attributed to the triplet state, with a strong dependence on substituent effects. The short-lived species of compound

2a, compared to compounds **1a** and **2b**, are associated with the existence of an intramolecular charge-transfer state (ICT). The nitro moiety in compounds **2c** and **1a** led to dominant non-radiative decay processes. The largest transient lifetime was presented by **1b**, due to its pronounced charge-transfer character. Solvent polarity also affected the photophysical properties, especially for **1b**, for which less polar solvents caused shorter λ_{max}^{T-T}, and τ values due to less effective stabilization of dipolar excited states and increased molecular flexibility. Photochemical reactivity was influenced by both the solvent and irradiation wavelength. Compounds **1a** and **1b** underwent photoreactions in MeOH, MeCN, and EtOAc; iminochalcone **2a** reacted in MeOH and EtOAc, whereas **2b** and **2c** were photoreactive exclusively in MeOH. Under Hg (Xe) lamp irradiation, **1a** presented spectral changes consistent with a $[2_\pi+2_\pi]$ photocycloaddition, while **1b** (in MeCN and EtOAc) underwent *E/Z*-photoisomerization. Under LED irradiation, both **1a** and **1b** were converted from *E*- to *Z*-isomer, as confirmed by ^{1}H NMR spectroscopy.

CRediT authorship contribution statement

Beatriz A. Riga-Rocha: Writing – original draft, Investigation. **José C. Netto-Ferreira:** Writing – review & editing, Formal analysis. **Carla C. Schmitt:** Supervision, Methodology, Conceptualization. **Antonio E.H. Machado:** Investigation, Formal analysis. **Thiago F. Silva:** Investigation.

Declaration of competing interest

The authors declare that they have no known competing financial interests or personal relationships that could have appeared to influence the work reported in this paper.

Acknowledgments

BARR is indebted to the financial support of CNPq (Conselho Nacional de Desenvolvimento Científico e Tecnológico, Brazil, Proc. 150759/2024-0) and CAPES (Coordenação de Aperfeiçoamento de Pessoal de Nível Superior, Brazil, Finance Code 001 and Proc. 1706422). CCS also thanks CNPq for research fellowship (Proc. 308880/2019-6 and 311184/2022-7). The authors would like to extend special thanks to Prof. Dr. Miguel G. Neumann for his support, wise advice, and invaluable experience, which he generously shared during the investigations and development of this work.

Appendix A. Supplementary data

Supplementary data to this article can be found online at https://doi.org/10.1016/j.jphotochem.2025.117005.

Data availability

Data will be made available on request.

References

[1] R. Mazumder, Ichudaule, A. Ghosh, S. Deb, R. Ghosh, Significance of chalcone scaffolds in medicinal chemistry, Top. Curr. Chem. 382 (2024) 1–22, 109, https://doi.org/10.1007/s41061-024-00468-7.
[2] W.J. Lee, J.C. Lim, S.-H. Paek, K. Song, J.Y. Chang, New photoreactive materials having chalcone units: synthesis and photoalignment of nematic liquid crystals, Korea Polym. J. 9 (2001) 339–344.
[3] S. Kobayashi, Y. Iimura, in: R. Shashidhar (Ed.), Surface liquid crystal molecular alignment in LCDs and their electro-optical performance, 1994, pp. 122–131, https://doi.org/10.1117/12.172114.
[4] S.-H. Paek, C.J. Durning, K.-W. Lee, A. Lien, A mechanistic picture of the effects of rubbing on polyimide surfaces and liquid crystal pretilt angles, J. Appl. Phys. 83 (1998) 1270–1280, https://doi.org/10.1063/1.366825.
[5] H.T. Kim, J.W. Lee, S.J. Sung, J.K. Park, Mechanism of photo-induced liquid crystal alignment on a poly(vinyl cinnamate) thin layer, Polym. J. 33 (2001) 9–12, https://doi.org/10.1295/polymj.33.9.
[6] D. Song, K. Jung, J. Moon, D. Shin, Photochemistry of chalcone and the application of chalcone-derivatives in photo-alignment layer of liquid crystal display, Opt. Mater. (Amst) 21 (2003) 667–671, https://doi.org/10.1016/S0925-3467(02)00220-3.
[7] K.G. Komarova, S.N. Sakipov, V.G. Plotnikov, M.V. Alfimov, Luminescent properties of chalcone and its aminoderivatives, JOL 164 (2015) 57–63, https://doi.org/10.1016/j.jlumin.2015.03.021.
[8] V.G. Plotnikov, Regularities of the processes of radiationless conversion in polyatomic molecules, Int. J. Quantum Chem. 16 (1979) 527–541, https://doi.org/10.1002/qua.560160311.
[9] K. Tokumura, K. Nagaosa, Y. Ohta, R. Matsushima, Temperature-dependent tautomer fluorescence spectra of 3′,4′-benzo-2′-hydroxychalcone: direct evidence for photoenolization followed by Z→E isomerization in the singlet manifold, Chem. Phys. Lett. 295 (1998) 516–524, https://doi.org/10.1016/S0009-2614(98)00984-1.
[10] Y. Kohno, M. Ito, M. Kurata, S. Ikoma, M. Shibata, R. Matsushima, Y. Tomita, Y. Maeda, K. Kobayashi, Photo-induced coloration of 2-hydroxychalcone in the clay interlayer, J. Photochem. Photobiol. A Chem. 218 (2011) 87–92, https://doi.org/10.1016/j.jphotochem.2010.12.007.
[11] P.E. Eaton, On the mechanism of the photodimerization of cyclopentenone, J. Am. Chem. Soc. 84 (1962) 2454–2455, https://doi.org/10.1021/ja00871a039.
[12] D. Cesarin-Sobrinho, J.C. Netto-Ferreira, R. Braz-Filho, Efeito da substituição por átomos de flúor no equilíbrio conformacional de chalcona, Quim Nova 24 (2001) 604–611, https://doi.org/10.1590/S0100-40422001000500006.
[13] X. Yuan, L. Men, Y. Liu, Y. Qiu, C. He, W. Huang, Truxillic and truxinic acid derivatives: configuration, source, and bioactivities of natural cyclobutane dimers, J. Holistic Integr. Pharm. 1 (2020) 48–69, https://doi.org/10.1016/S2707-3688(23)00039-0.
[14] T. Arai, K. Tokumaru, Photochemical one-way adiabatic isomerization of aromatic olefins, Chem. Rev. 93 (1993) 23–39, https://doi.org/10.1021/cr00017a002.
[15] T. Arai, T. Karatsu, H. Sakuragi, K. Tokumari, "One-way" photoisomerization between cis- and trans-olefin. A novel adiabatic process in the excited state, Tetrahedron Lett. 24 (1983) 2873–2876, https://doi.org/10.1016/S0040-4039(00)88047-8.
[16] D.H. Waldeck, Photoisomerization dynamics of stilbenes, Chem. Rev. 91 (1991) 415–436, https://doi.org/10.1021/cr00003a007.
[17] B.A. Riga-Rocha, A.E.H. Machado, M.G. Neumann, C.C.S. Cavalheiro, Experimental and theoretical study of three newly-synthesized iminochalcones: An example of dual emission induced by polarity changes, J. Photochem. Photobiol. A Chem. 426 (2022) 113725, https://doi.org/10.1016/j.jphotochem.2021.113725.
[18] E. Stadler, A. Eibel, D. Fast, H. Freißmuth, C. Holly, M. Wiech, N. Moszner, G. Gescheidt, A versatile method for the determination of photochemical quantum yields via online UV-vis spectroscopy, Photochem. Photobiol. Sci. 17 (2018) 660–669, https://doi.org/10.1039/c7pp00401j.
[19] M.J. Frisch, G.W. Trucks, H.B. Schlegel, G.E. Scuseria, J.R. Robb M. A. and Cheeseman, G. Scalmani, V. Barone, B. Mennucci, H. Petersson G. A. and Nakatsuji, M. Caricato, X. Li, H.P. Hratchian, J. Izmaylov A. F. and Bloino, G. Zheng, J.L. Sonnenberg, M. Hada, M. Ehara, R. Toyota K. and Fukuda, J. Hasegawa, M. Ishida, T. Nakajima, Y. Honda, H. Kitao O. and Nakai, T. Vreven, J.A.Jr. Montgomery, J.E. Peralta, M. Ogliaro F. and Bearpark, J.J. Heyd, E. Brothers, K.N. Kudin, T. Staroverov V. N. and Keith, R. Kobayashi, J. Normand, K. Raghavachari, J.C. Rendell A. and Burant, S.S. Iyengar, J. Tomasi, M. Cossi, J.M. Rega N. and Millam, M. Klene, J.E. Knox, J.B. Cross, C. Bakken V. and Adamo, J. Jaramillo, R. Gomperts, R.E. Stratmann, A.J. Yazyev O. and Austin, R. Cammi, C. Pomelli, J.W. Ochterski, K. Martin R. L. and Morokuma, V.G. Zakrzewski, G.A. Voth, J.J. Salvador P. and Dannenberg, S. Dapprich, A.D. Daniels, J.B. Farkas O. and Foresman, J. V Ortiz, J. Cioslowski, D.J. Fox, Gaussian 09, Revision E.01, (2013).
[20] J. Tirado-Rives, W.L. Jorgensen, Performance of B3LYP density functional methods for a large set of organic molecules, J. Chem. Theory Comput. 4 (2008) 297–306, https://doi.org/10.1021/ct700248k.
[21] N. Godbout, D.R. Salahub, J. Andzelm, E. Wimmer, Optimization of Gaussian-type basis sets for local spin density functional calculations. Part I. Boron through neon, optimization technique and validation, Can. J. Chem. 70 (1992) 560–571, https://doi.org/10.1139/v92-079.
[22] C. Sosa, J. Andzelm, B.C. Elkin, E. Wimmer, K.D. Dobbs, D.A. Dixon, A local density functional study of the structure and vibrational frequencies of molecular transition-metal compounds, J. Phys. Chem. 96 (1992) 6630–6636, https://doi.org/10.1021/j100195a022.
[23] F. Neese, Software update: the ORCA program system—version 6.0, WIREs Comput. Mol. Sci. 15 (2025) 1–10, https://doi.org/10.1002/wcms.70019.
[24] F. Neese, F. Wennmohs, U. Becker, C. Riplinger, The ORCA quantum chemistry program package, J. Chem. Phys. 152 (2020) 224108, https://doi.org/10.1063/5.0004608.
[25] A. Hellweg, D. Rappoport, Development of new auxiliary basis functions of the Karlsruhe segmented contracted basis sets including diffuse basis functions (def2-SVPD, def2-TZVPPD, and def2-QVPPD) for RI-MP2 and RI-CC calculations, Phys. Chem. Chem. Phys. 17 (2015) 1010–1017, https://doi.org/10.1039/C4CP04286G.
[26] F. Weigend, R. Ahlrichs, Balanced basis sets of split valence, triple zeta valence and quadruple zeta valence quality for H to Rn: design and assessment of accuracy, Phys. Chem. Chem. Phys. 7 (2005) 3297–3305, https://doi.org/10.1039/b508541a.
[27] F. Weigend, Accurate Coulomb-fitting basis sets for H to Rn, Phys. Chem. Chem. Phys. 8 (2006) 1057–1065, https://doi.org/10.1039/b515623h.
[28] S. Grimme, F. Neese, Double-hybrid density functional theory for excited electronic states of molecules, J. Chem. Phys. 127 (2007) 154116, https://doi.org/10.1063/1.2772854.

[29] M. Casanova-Páez, M.B. Dardis, L. Goerigk, ωB2PLYP and ωB2GPPLYP: the first two double-hybrid density functionals with long-range correction optimized for excitation energies, J. Chem. Theory Comput. 15 (2019) 4735–4744, https://doi.org/10.1021/acs.jctc.9b00013.
[30] M. Casanova-Páez, L. Goerigk, Time-dependent long-range-corrected double-hybrid density functionals with spin-component and spin-opposite scaling: a comprehensive analysis of singlet–singlet and singlet–triplet excitation energies, J. Chem. Theory Comput. 17 (2021) 5165–5186, https://doi.org/10.1021/acs.jctc.1c00535.
[31] M. Garcia-Ratés, F. Neese, Effect of the solute cavity on the solvation energy and its derivatives within the framework of the Gaussian charge scheme, J. Comput. Chem. 41 (2020) 922–939, https://doi.org/10.1002/jcc.26139.
[32] M. Cossi, N. Rega, G. Scalmani, V. Barone, Energies, structures, and electronic properties of molecules in solution with the C-PCM solvation model, J. Comput. Chem. 24 (2003) 669–681, https://doi.org/10.1002/jcc.10189.
[33] Y. Xue, J. Mou, Y. Liu, X. Gong, Y. Yang, L. An, An ab initio simulation of the UV/visible spectra of substituted chalcones, Open Chem. 8 (2010) 928–936, https://doi.org/10.2478/s11532-010-0058-3.
[34] T.A. Fayed, M.K. Awad, Dual emission of chalcone-analogue dyes emitting in the red region, Chem. Phys. 303 (2004) 317–326, https://doi.org/10.1016/j.chemphys.2004.06.023.
[35] C. Reichardt, T. Welton, Solvents and Solvent Effects in Organic Chemistry, fourth ed, Wiley-VCH, Weinheim, 2010, pp. 550–552, https://doi.org/10.1002/9783527632220.
[36] H. Gruen, H. Goerner, Trans → cis photoisomerization, fluorescence, and relaxation phenomena of trans-4-nitro-4′-(dialkylamino)stilbenes and analogues with a nonrotatable amino group, J. Phys. Chem. 93 (1989) 7144–7152, https://doi.org/10.1021/j100357a024.
[37] Y.M. Poronik, G.V. Baryshnikov, I. Deperasińska, E.M. Espinoza, J.A. Clark, H. Ågren, D.T. Gryko, V.I. Vullev, Deciphering the unusual fluorescence in weakly coupled bis-nitro-pyrrolo[3,2-b]pyrroles, Commun. Chem. 3 (2020) 190, https://doi.org/10.1038/s42004-020-00434-6.
[38] G. Engler, M. Nispel, C. Marian, K. Kleinermanns, Transient spectroscopy of UV excited flavone: triplet-triplet absorption and comparison with theory, Chem. Phys. Lett. 473 (2009) 167–170, https://doi.org/10.1016/j.cplett.2009.03.051.
[39] R.A. Caldwell, M. Singh, Effect of a polar substituent on olefin triplet lifetime, J. Am. Chem. Soc. 105 (1983) 5139–5140, https://doi.org/10.1021/ja00353a051.
[40] I. Carmichael, G.L. Hug, Triplet–Triplet Absorption Spectra of Organic Molecules in Condensed Phases, J. Phys. Chem. Ref. Data Monogr. 15 (1986) 1–250. Doi: https://doi.org/10.1063/1.555770.
[41] X. Allonas, C. Ley, C. Bibaut, P. Jacques, J.P. Fouassier, Investigation of the triplet quantum yield of thioxanthone by time-resolved thermal lens spectroscopy: solvent and population lens effects, Chem. Phys. Lett. 322 (2000) 483–490, https://doi.org/10.1016/S0009-2614(00)00462-0.
[42] Z.R. Grabowski, K. Rotkiewicz, W. Rettig, Structural changes accompanying intramolecular electron transfer: focus on twisted intramolecular charge-transfer states and structures, Chem. Rev. 103 (2003) 3899–4031, https://doi.org/10.1021/cr940745l.
[43] M. Takezaki, N. Hirota, M. Terazima, Nonradiative relaxation processes and electronically excited states of nitrobenzene studied by picosecond time-resolved transient grating method, J. Phys. Chem. A 101 (1997) 3443–3448, https://doi.org/10.1021/jp963095t.
[44] B.S. Al-Saadi, A.R. Ibrahim, J. Husband, A.H. Ismail, Y. Baqi, O.K. Abou-Zied, Enhanced intramolecular charge transfer and near-infrared fluorescence in 4-dimethylamino-chalcone analogues through extended conjugation: synthesis, photophysical properties, and theoretical modelling, Phys. Chem. Chem. Phys. 26 (2024) 12844–12851, https://doi.org/10.1039/D4CP00289J.
[45] J. Suresh, S. Karthik, A. Arun, Cis–trans isomerism shown by the polymer containing chalcone moiety in its side chain, Polym. Adv. Technol. 27 (2016) 1274–1283, https://doi.org/10.1002/pat.3791.
[46] Z.K. Si, Q. Zhang, M.Z. Xue, Q.R. Sheng, Y.G. Liu, Novel UV-sensitive bis-chalcone derivatives: synthesis and photocrosslinking properties in solution and solid PMMA film, Res. Chem. Intermediat. 37 (2011) 635–646, https://doi.org/10.1007/s11164-010-0236-0.
[47] R. Balaji, S. Nanjundan, Synthesis and characterization of photocrosslinkable functional polymer having pendant chalcone moiety, React. Funct. Polym. 49 (2001) 77–86, https://doi.org/10.1016/S1381-5148(01)00062-1.
[48] B. Mani, S. Kathavarayan, Studies on photocrosslinking and flame-retardant properties of chalcone-based polyacrylamides, Polym. Adv. Technol. 27 (2016) 466–476, https://doi.org/10.1002/pat.3692.
[49] A. Rehab, N. Salahuddin, Photocrosslinked polymers based on pendant extended chalcone as photoreactive moieties, Polymer 40 (1999) 2197–2207, https://doi.org/10.1016/S0032-3861(98)00460-1.
[50] B. Ramaganthan, M. Gopiraman, L.O. Olasunkanmi, M.M. Kabanda, S. Yesudass, I. Bahadur, A.S. Adekunle, I.B. Obot, E.E. Ebenso, Synthesized photo-cross-linking chalcones as novel corrosion inhibitors for mild steel in acidic medium: experimental, quantum chemical and Monte Carlo simulation studies, RSC Adv. 5 (2015) 76675–76688, https://doi.org/10.1039/c5ra12097g.
[51] T. Maldonado, F. Godoy, G. Ferraudi, A. Graham Lappin, On the photochemical properties of the organometallic trans cyrhetrenyl chalcone (E). Deceleration of the photoisomerization and quenching of the luminescence effected by the photogenerated cis isomer (Z), Inorg. Chim. Acta 469 (2018) 239–244, https://doi.org/10.1016/j.ica.2017.09.022.
[52] T. Maldonado, G. Ferraudi, A.G. Lappin, F. Godoy, Kinetic and mechanistic observations on the photoinduced isomerization reaction of organometallic chalcones: a steady state and flash photolysis study, ChemPhotoChem 2 (2018) 95–104, https://doi.org/10.1002/cptc.201700129.
[53] S.N. Sidharth, A.R. Yuvaraj, T.J. Hui, B.K. Sarojini, M.Y. Mashitah, G. Hegde, Light induced properties of chalcones correlated with molecular structure and photophysical properties for permanent optical storage device, Adv. Mat. Res. 1033–1034 (2014) 1149–1153, https://doi.org/10.4028/www.scientific.net/AMR.1033-1034.1149.
[54] D.-M. Shin, D.-M. Song, K.-H. Jung, J.-H. Moon, Photochemical transformation of chalcone derivatives, J. Photosci. 8 (2001) 9–12.
[55] H. Furuuchi, T. Arai, Y. Kuriyama, H. Sakuragi, K. Tokumaru, Factors distinguishing one-way and two-way photoisomerization of aromatic olefins. Effects of substituents on triplet energy surfaces of 8-fluoranthenylethylenes, Chem. Phys. Lett. 162 (1989) 211–216, https://doi.org/10.1016/0009-2614(89)85126-7.
[56] H.E. Zimmerman, H. Iwamura, Thermal and photochemical interconversions of cyclooctatetraenes and semibullvalenes. Exploratory organic photochemistry. LII, J. Am. Chem. Soc. 92 (1970) 2015–2022, https://doi.org/10.1021/ja00710a038.
[57] B.E. Aksöz, R. Ertan, Chemical and structural properties of Chalcones I, J. Pharm. Sci. 36 (2011) 223–242.
[58] B.E. Aksöz, R. Ertan, Spectral properties of Chalcones II, J. Pharm. Sci. 37 (2012) 205–216.
[59] S.K. Yazdan, V. Sagar, A.B. Shaik, Chemical and biological potentials of Chalcones: a review, Org. Med. Chem. Int. J. 1 (2015) 1–9.
[60] R. Nagwanshi, M. Bakhru, S. Jain, Photodimerization of heteroaryl chalcones: comparative antimicrobial activities of chalcones and their photoproducts, Med. Chem. Res. 21 (2012) 1587–1596, https://doi.org/10.1007/s00044-011-9667-4.
[61] T. Lei, C. Zhou, M. Huang, L. Zhao, B. Yang, C. Ye, H. Xiao, Q. Meng, V. Ramamurthy, C. Tung, L. Wu, General and efficient intermolecular [2+2] photodimerization of chalcones and cinnamic acid derivatives in solution through visible-light catalysis, Angew. Chem. Int. Ed. 129 (2017) 15609–15612, https://doi.org/10.1002/ange.201708559.